INSTRUMENTATION

A Measure of Anger-Camera Linearity: Results With and Without a Corrector

Kenneth F. Koral, Mark E. Schrader, and Glenn F. Knoll

Medical Data Systems, Ann Arbor, Michigan

A method for measuring the X and Y linearity of an Anger camera coupled to a computer is presented. It has similarities to, and differences from, the method recommended by the National Electrical Manufacturers Association (NEMA). Test images are taken through a lead plate with parallel and equally spaced slots, and the locations of the lines in the images are fitted by least-squares with an equation that allows for slight misalignment. Discrepancies from the fit are calculated and displayed as a distribution over the camera field. The maximum and average discrepancies are tabulated. The field of view that is of interest is selectable within the analysis program.

Among four large-field-of-view uncorrected cameras, three 37-tube types (two measured using Tc-99m and one with Au-195) show a similar degree of nonlinearity. However, the maximum and average discrepancies from linearity for a 61-tube prototype camera, measured using Tc-99m over a 15-in. field of view, are 40% of those for the other three. For the four cameras, an event-shifting on-line corrector with best-case sampling improves linearity by an average factor of 5.5, including both 15- and 11.25-in. fields of view.

To define spatial linearity of an Anger camera, consider the following hypothetical experiment. Illuminate the camera with two point sources that are separated by a given distance and whose gamma rays are well collimated for normal incidence. Record an image. Move the point-source pair to any other position, maintaining the same separation. Make another image. Repeat indefinitely. The camera has a linear spatial response if the resulting pairs of recorded point sources have the same separation in all images. Effects on recorded location due to non-normal incidence, which have recently been reported (*1*), are excluded from consideration in this paper.

Spatial nonlinearity exists to a measurable extent in all present-day cameras. It is, moreover, the major cause of nonuniformity in Anger-camera flood images, as reported by Wicks and Blau (*2*). And such nonlinearity is potentially an important degrading factor in transverse emission computed tomography wherein quantitatively accurate projections are assumed when the reconstruction process is carried out. Normalization (with a field-flood phantom) is designed to correct nonuniformity—the result of nonlinearity—when the projected object is uniform. Although such normalization can have beneficial effects in tomography (*3*), it seems obvious that only true correction will completely restore the data in all cases.

In this paper we present a method for measuring linearity that is applicable to any Anger camera coupled to a computer. The method is similar to that recommended by the National Electrical Manufacturers Association (NEMA) standards (*4*). The points of agreement with the NEMA standard method are:

1. The X and Y linearity are measured separately.

2. A lead plate with parallel, equally spaced slots is required.

3. A best set of parallel, equally spaced lines is fitted to the data.

The points of disagreement are:

1. The fitting equation involves three parameters, so that slight misalignment of the plate with respect to the camera axes can be taken into account.

2. The maximum and average discrepancies of the line locations from the fitting-equation values are given as a measure of absolute linearity, rather than maximum discrepancy only.

3. No measure of differential linearity is presented.

4. A display of the magnitude and sign of the discrepancy over the field of view is given.

5. We vary the size of the field of view that is of interest and carry out the analysis for each size, whereas under the NEMA standards one does a single fit and reports the discrepancies over the entire field of view and over a smaller, included region.

Results for uniformity, but not linearity, using the NEMA method have been given by Muehllehner et al. (5) for a Searle* LFOV camera with and without a linearity corrector.

Herein we present linearity results for four large-field-of-view cameras including the Searle. In addition to the general method for measuring linearity and the results from it for the four cameras, we also present the results for these cameras when they are coupled to a microprocessor-based, on-line linearity corrector (6) developed by Medical Data Systems (MDS). This corrector is of the type that repositions events, based upon a calibration, without adding or subtracting any counts. To determine the true X coordinate, a double linear interpolation is carried out using four stored "corner" values that are indexed by the apparent X-Y coordinates. The true Y coordinate is determined in a similar way. Up
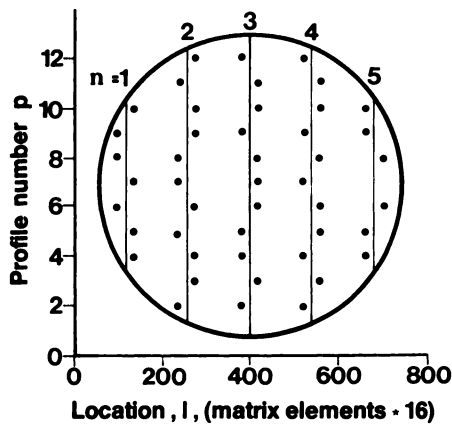

FIG. 1. Diagram illustrating algorithm for an imaginary camera covered by only five lines and 12 profiles (instead of 19 and 64, respectively). Dots are locations of lines in data image at each profile level. Equally spaced and parallel lines are hypothetical results of least-squares fit. Errors, $\Delta_{n,p}$, are distances from points to the corresponding line.
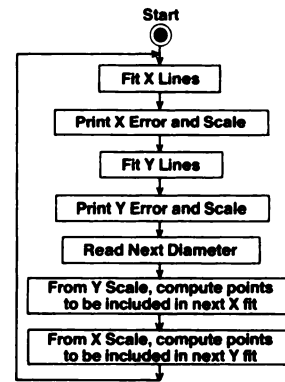

FIG. 2. Flow chart for calculating linearity measure as a function of diameter of field of view of interest. Note that fit and error are recalculated each time diameter is changed, so that region of camera outside the field of view of interest is ignored. If the error had simply been recalculated, as in the NEMA standards, then results would be a measure of distribution of error over a 15-in.-diameter field of view. This is done in this paper with a distribution display (Fig. 5).

to a count rate of 120,000/sec, the time of this calculation should not introduce additional dead time.

PROCEDURE

Data. All cameras are actually connected to the MDS corrector for all tests. However, the corrector is placed in one of two modes: (1) A mode wherein the X and Y signals are passed through without any change; this we will call corrector-off. (2) A mode wherein the X and Y signals activate the translation-table lookup and thus start the process for producing a corrected X-Y pair. This mode we will call corrector-on. In both modes, the corrector verifies that the total-energy signal for the event is within a floating (that is, spatially variant) pulse-height window before the event is passed. The table in the corrector that specifies this window has previously been filled by an energy calibration. By using the above procedure, the only difference between the two results is the activation of spatial correction. Moreover, all the comments below on the corrector-off mode should apply to measurements on a camera coupled directly to a computer (the floating pulse-height window is not expected to have a large effect on linearity.).

The plates used are lead, ⅛ in. thick, on an aluminum backing. Slots ⅛ in. wide are milled in these plates with a center-to-center spacing of 0.76 in. (This width and spacing are, incidentally, different from those called for in the NEMA standards). Nineteen slots fall within a 15-in. field of view.

The procedure is to remove the collimator and place the plate on the camera with the slots running perpendicular to the X direction. The camera is then presented with a point source placed about 2 m away, so that detected events are from photons entering the crystal with near-normal incidence. One or more 128 × 128 images
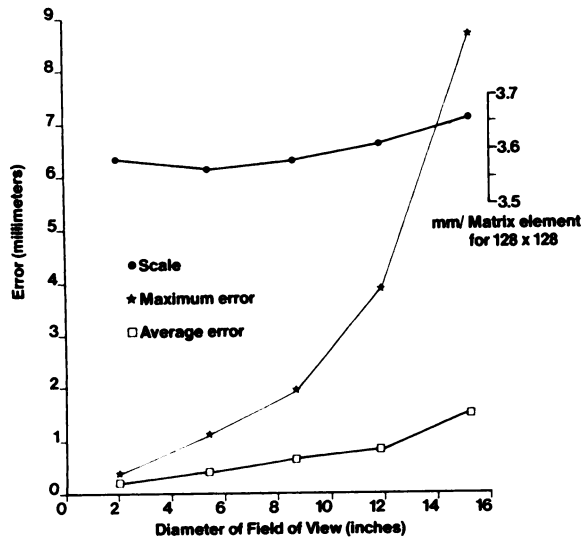
1070

FIG. 3. Comparison of maximum error with average error for X linearity, as a function of field diameter. Scale value resulting from each fit is shown at top. Camera is a Searle LFOV presented with Au-195 (99 keV).

are stored in the computer. The plate is then rotated 90° and a second, Y-linearity image set is recorded.

The above procedure provides the data needed by the linearity algorithm described in the next section. For this paper, all data are effectively taken twice, once with the corrector on and once with it off. The cameras are actually first put through the full corrector calibration procedure. In fact, the procedure for calibrating the camera is the same as that for measuring the camera's linearity. Thus saved calibration data can be, and in some cases are, used for corrector-off data.

Algorithm. The first step in handling the data is to ascertain the location of each of the image's lines that corresponds to the slot in the plate at each of 64 profiles through the image. A "centroid" or "center of gravity" calculation is performed on the peaks in the profile p, and the locations $l_{n,p}$ are found and saved to a precision of 1 part in 2048. Here n is the line number index. These locations are plotted as the black dots in Fig. 1.

The next step is to do a least-squares fit to a set of lines that are equally spaced and parallel but are allowed to have a slight angle with the coordinate axis so that there is a dependence on profile number. The equation for this set of lines is given by

$$l = A + Bn + Cp$$

where l is the peak location and has the units (matrix elements) *16 and A, B, and C are the fitting constants to be determined. Calculation of the least-squares fit to the data involves inversion of a 3 × 3 matrix, the details of which are given in Appendix I. After the fit, A represents an offset, 16*(19.34 mm)/B is the scale in mm/matrix element for a 128 × 128 image, and C is near zero but accounts for the line plate's being not perfectly aligned. The lines then fall on the graph as

shown in Fig. 1.

The final step is to evaluate the discrepancy $\Delta_{n,p}$ between the fit and the data for each of the locations:

$$\Delta_{n,p} = l_{n,p} - l.$$

The maximum of the absolute values of these discrepancies, Δ_{max}, is max ($|\Delta_{n,p}|$). The average $\overline{\Delta}$ of the absolute values is

$$\frac{1}{N} \Sigma \ |\Delta_{n,p}|$$

Here N is the total number of data points for the given field of view.

The flow chart for carrying out the calculation as a function of the field of view is shown in Fig. 2. The center of the image is an input parameter. For successive calculations, smaller and smaller subsets of the original data are used in fitting lines and calculating errors. The points to be included in each pass are those lying within the radius of a synthesized circular field of view. The previously evaluated scale in the profile direction relates profile number to distance. Thereby, a circular mask of given diameter can be laid over the available points to help choose those within the designated field.

At each diameter, one can view a display of the discrepancy from linearity as distributed over the camera face, calculated by interpolation from the values for each line. For the image, a distortion in the direction toward the central line is displayed as brighter than the no-error intensity, and a distortion in the opposite direction as darker than the no-error intensity, which is itself shown
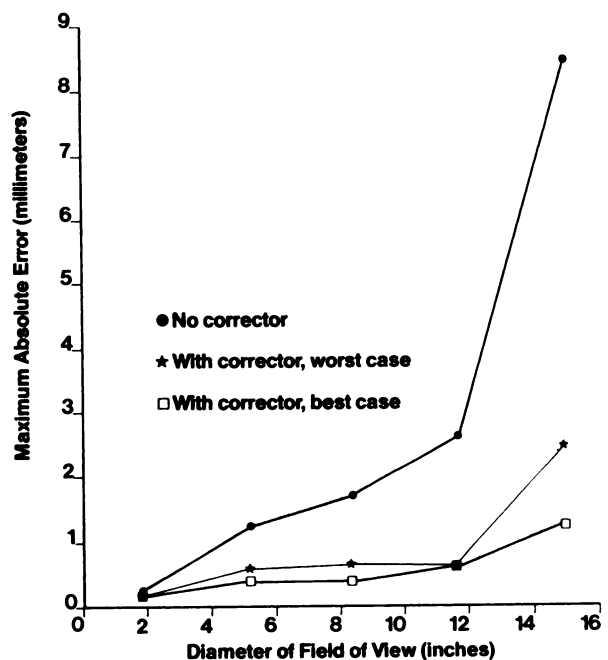

FIG. 4. Plot of maximum absolute X errors as a function of field diameter, with and without MDS corrector. Best- and worst-case sampling are explained in text. Camera is a GE 400T presented with Tc-99m.

TABLE 1. COMPARISON OF LINEARITY WITH CORRECTOR ON BETWEEN BEST- AND WORST-CASE SAMPLING

	Maximum error (mm)				Average error (mm)			
	X linearity		Y linearity		X linearity		Y linearity	
Case	UFOV*	CFOV†	UFOV	CFOV	UFOV	CFOV	UFOV	CFOV
Best	1.3	0.54	1.4	0.59	0.20	0.12	0.20	0.13
Worst	2.5	0.59	2.6	0.62	0.27	0.18	0.23	0.15

* UFOV = useful field of view, 15 in.

† CFOV = central field of view, 11.25 in.

in a corner of the image.

RESULTS

Plots of maximum error and average error against field of view are shown in Fig. 3 for a 1978 Searle LFOV camera with corrector off, using the emitter Au-195. It is seen that at 15 in. the maximum error (8.5 mm) is more than five times the average error (1.5 mm), emphasizing the need for a clear definition of what has been measured when camera linearity is discussed. The scale as given by the least-squares fitting is also plotted. This scale is an integral one, so it does not vary as fast with diameter as a local scale would. However, the scale shown changes by 2.6% between 5.25 and 15 in., whereas with the corrector on (not shown) the variation is 0.1%.

The effect of the linearity corrector on maximum error is shown in Fig. 4 for a GE 400T camera and Tc-99m. The shape of the corrector-off curve is similar to that for maximum error for the Searle camera. At a 15-in. field of view the improvement with the corrector on is a factor of 3 for the "worst-case" sampling and a factor of 6 for the "best-case" sampling.

The meanings of best case and worst case are as follows. Since the same line plate in about the same position is used for the linearity test and for the corrector's linearity calibration, the sampling in the corrector-on test is somewhat favorable. In the case of this camera, we displaced the plate a distance equal to half the line spacing, thus requiring the greatest interpolation from the corrector, and took a second measure of linearity, which we will call worst case. The best- and the worst-case results are both plotted in Fig. 4, and are given in Table 1 for both X and Y linearity and maximum and average error. They are tabulated for a useful field of view (UFOV) of 15 in. and for a central field of view (CFOV) of 11.25 in.—75% of the UFOV diameter. As shown by the graph and table, the difference between best case and worst case can be as much as a factor of 2 but it is usually less than that. We feel that the difference is not so large that the best-case results misrepresent the ideal situation wherein some type of average between best and worst case would be used. Therefore, except as noted, best-case results will be presented from here on in this paper.

For the GE 400T camera, Fig. 5 is a comparison of the distribution of error as a function of camera position for X and Y linearity, with the corrector both on and off. With the corrector off, the error at the edges is large and toward the midline. Also, the pattern of error is such that
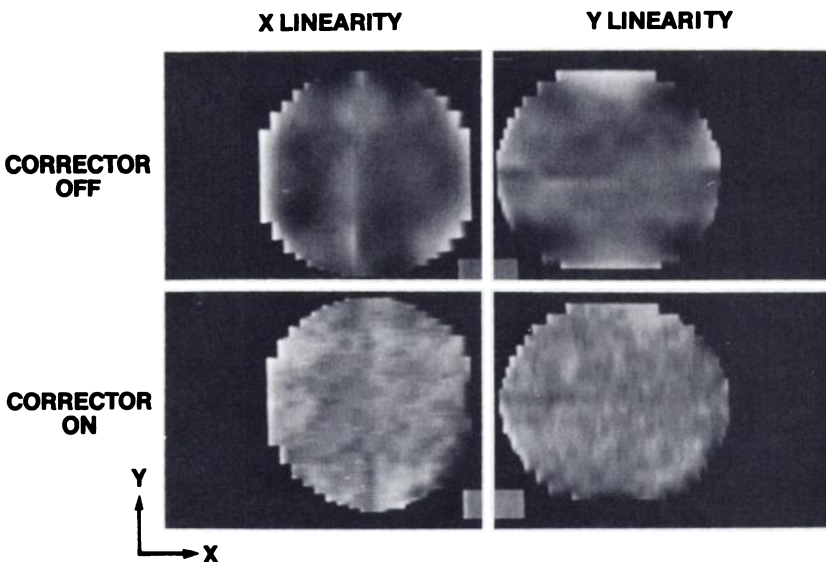

FIG. 5. Distributions of nonlinearity as a function of position for a GE 400T camera, with and without MDS corrector. Intensity corresponding to no error is shown in the corner of each image. Intensities brighter than this correspond to distortion toward a line through center of camera and perpendicular to the axis for which the linearity is shown (X or Y). Darker intensities correspond to distortion away from this central line. With corrector off there are large regions of similar distortion, whereas with corrector on the remaining distortion is randomly distributed. Note that since each image is self-normalized, one cannot compare the brightness or darkness of one image with another in order to compare distortion. See Tables 2 and 3 to carry out such comparison.
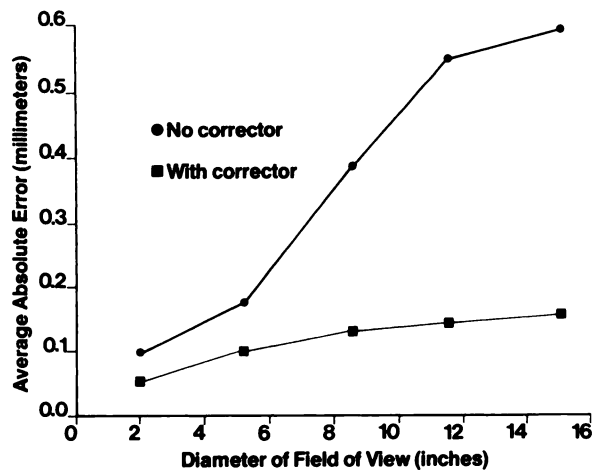
FIG. 6. Plot of average error over field of view for X linearity as a function of field diameter, with and without MDS corrector. Camera is a GE 61-tube prototype; source is Tc-99m. Here, without corrector, error is approximately linearly dependent upon diameter all the way out to 15 in., in contrast with other cameras (see example in Fig. 3).

large regions exhibit similar error. With the corrector on, the error is much more randomly distributed, probably representing randomly distributed calculational error. The dark areas at the right of the X-linearity image and at the bottom of the Y-linearity image represent two areas of the camera where the correction algorithm had relative difficulty. Note that the images in Fig. 5 are each self-normalized, so that one cannot compare intensity differences between the images to get a comparison of relative nonlinearity.

Figure 6 is a plot of average error for a preproduction model of a GE 61-tube camera presented with Tc-99m. The shape of the corrector-off curve is somewhat different in this case, with an almost linear dependence of the error upon diameter.

Again, with the corrector on, the linearity is improved at all diameters, with the corrector-on error being only one-fifth as large as the corrector-off error at 15 in.

A camera-to-camera comparison is shown in Tables 2 and 3. Note that the Searle camera is measured with Au-195, whose energy (99 keV) is lower than the 140 keV used for the other cameras. The lower energy could

affect the linearity, but we do not expect the effect to be large enough to alter our general conclusions. The results for X and Y linearity are quite similar. Among camera results, the GE 61-tube is superior, especially when one considers maximum error or when one is interested in a field of view of 15 in. (UFOV). A large improvement with the corrector on occurs in all cases.

DISCUSSION

Inspection of the uniformity of a field-flood image tells one a considerable amount about the quality of a camera's linearity. The uniformity of such flood images, however, is quite difficult to quantify (4,7), so we have pursued a direct measure of camera linearity by investigating the output image when the camera is presented with straight and equally spaced lines. With this method, quantitative answers for a given camera could depend on the line spacing, line placement, and definition of the field of view, as all of these affect exactly where the camera's linearity is being sampled. Without the corrector on, we expect the location of the lines to have a small effect on the result, and we have treated all cameras tested in approximately the same way to make the results unprejudiced. With the corrector on, we have defined the differences caused by line displacement. The method for finding the field of view in this paper has been well specified.

We recommend the inclusion of the average nonlinearity statistic in the NEMA standards. The maximum nonlinearity, given by a single discrepancy, reflects the condition at a single region or type of region (field edges) of the camera. Meanwhile, the average discrepancy gives a measure of the nonlinearity of the camera as a whole over the field of view. Similarly, we prefer the use of a fitting equation that allows for slight misalignment of the line plate with respect to the coordinate axes without penalizing the linearity results. This, we feel, is an improvement over the NEMA standard method, but we have not estimated the magnitude of the effect of this misalignment upon linearity. Finally, it is our opinion that redoing the calculation for different fields of view is an improvement on the standards, although this procedure does take longer.

TABLE 2. COMPARISON OF MAXIMUM ERROR AMONG FOUR CAMERAS

Camera	X linearity (mm)				Y linearity (mm)			
	Uncorrected		Corrected		Uncorrected		Corrected	
	UFOV*	CFOV†	UFOV	CFOV	UFOV	CFOV	UFOV	CFOV
Picker DC 4/15	9.4	4.2	1.4	0.34	6.3	2.7	1.6	0.49
GE 400T	8.4	2.5	1.2	0.54	6.8	2.6	1.4	0.59
GE 61-tube	2.8	1.8	0.84	0.39	2.7	1.7	1.2	0.53
Searle	8.5	3.6	1.2	0.54	6.3	2.7	1.6	0.49

* UFOV = useful field of view, 15 in.
† CFOV = central field of view, 11.25 in.

TABLE 3. COMPARISON OF AVERAGE ERROR AMONG FOUR CAMERAS

Camera	X linearity (mm)				Y linearity (mm)			
	Uncorrected		Corrected		Uncorrected		Corrected	
	UFOV*	CFOV†	UFOV	CFOV	UFOV	CFOV	UFOV	CFOV
Picker DC 4/15	1.2	0.82	0.14	0.11	1.4	0.94	0.16	0.10
GE 400T	1.5	0.60	0.20	0.12	1.5	0.67	0.20	0.13
GE 61-tube	0.59	0.51	0.12	0.11	0.63	0.51	0.12	0.11
Searle	1.5	0.78	0.21	0.17	1.1	0.56	0.26	0.23

* UFOV = useful field of view, 15 in.
† CFOV = central field of view, 11.25 in.

CONCLUSIONS

(1) Anger-camera linearity can be measured as a function of the diameter of the field of view of interest.

(2) For a 15-in.-diam field of view, maximum error among four uncorrected large-field-of-view cameras is larger than average error by a factor of from 5 to 8.

(3) The three uncorrected 37-tube cameras studied are roughly comparable. However, at a field of 15 in., the maximum and average distortions in the uncorrected 61-tube prototype camera show an average combined improvement factor of 2.5 over the three 37-tube cameras.

(4) The MDS event-shifting, on-line corrector improves linearity in all cases. The gain between corrector-off and best-case-sampling corrector-on results is a factor of 5.5 when averaged over 15- and 11.25-in. fields of view, maximum and average error, and four different cameras.

(5) For a GE 400T camera with the corrector on, the distortion results for best- and worst-case sampling differ by at most a factor of 2.

FOOTNOTE

* Now Siemen's Gammasonics, Inc.

APPENDIX I

The set of line locations is given by $l_{n,p}$, where p is the profile number running from 1 to 64, and n is the line number index running from n_{min} to n_{max}, where n_{min} lies between 1 and 11 and n_{max} between 11 and 21, with actual values determined by the profile of interest. The fitting equation that allows the set of equally spaced, parallel lines to have a slight angle with the coordinate axis is

$$l = A + Bn + Cp.$$

Then the function F to be minimized for a least-squares fit is

$$F = \sum(A + Bn + Cp - l_{n,p})^2,$$

where $\sum$ represents a double summation over p from 1 to 64 and over n from n_{min} to n_{max}. Differentiation of F with respect to A, B, and C in turn leads to three equations in three unknowns, which can be written in matrix form as

$$\begin{bmatrix} N & \sum n & \sum p \\ \sum n & \sum n^2 & \sum np \\ \sum p & \sum np & \sum p^2 \end{bmatrix} \begin{bmatrix} A \\ B \\ C \end{bmatrix} = \begin{bmatrix} \sum l_{n,p} \\ \sum n l_{n,p} \\ \sum p l_{n,p} \end{bmatrix}$$

Call the above matrix M. The values of A, B, and C are found by taking the inverse of M by standard techniques. Then

$$\begin{bmatrix} A \\ B \\ C \end{bmatrix} = M^{-1} \begin{bmatrix} \sum l_{n,p} \\ \sum n l_{n,p} \\ \sum p l_{n,p} \end{bmatrix}.$$

REFERENCES

1. SHABASON L, LeFREE MT, KIRCH DL, et al: Energy and angular dependent distortions in Anger camera images. *J Nucl Med* 21:P81,1980 (abst)
2. WICKS R, BLAU M: Effect of spatial distortion on Anger camera field-uniformity correction: Concise communication. *J Nucl Med* 20:252-254, 1979
3. JASZCZAK RJ, COLEMAN RE: Selected processing techniques for scintillation camera based SPECT systems. *Single Photon Emission Computed Tomography and Other Selected Computer Topics*. J. A. Sorenson, Ed. New York, Society of Nuclear Medicine, 1980, pp 45-59
4. Standards Publication No. NU1-1980. Performance measurements of scintillation cameras. Washington, DC, National Electrical Manufacturers Association (NEMA), 1980
5. MUEHLLEHNER G, COLSHER JG, STOUB EW: Correction for field nonuniformity in scintillation cameras through removal of spatial distortion. *J Nucl Med* 21:771-776, 1980
6. KNOLL GF, BENNETT MC, KORAL KF, et al: Removal of gamma camera nonlinearity and nonuniformities through real-time signal processing. *Proceedings of VI International Conference on Information Processing in Medical Imaging*. Paris, INSERM, 1979, Vol. 88, pp 187-200
7. MUEHLLEHNER G, WAKE RH, SANO R: Standards for performance measurements in scintillation cameras. *J Nucl Med* 22:72-72-77, 1981